Cloud Publications
International Journal of Advanced Remote Sensing and GIS
2015, Volume 4, Issue 1, pp. 1142-1160, Article ID Tech-429
ISSN 2320 - 0243

Research Article **Open Access**

Approximation of Flow Patterns for Submarine Channel Systems in the Arabian Sea using a GIS Approach

Prerna Ramesh, Dhananjai Kumar Pandey and Ravi Mishra

National Centre for Antarctic and Ocean Research, Headland Sada, Vasco-da-Gama, Goa, India

Correspondence should be addressed to Prerna Ramesh, prerna.geoinfo@gmail.com

Publication Date: 27 July 2015

Article Link: http://technical.cloud-journals.com/index.php/IJARSG/article/view/Tech-429

Abstract The Indus fan in the Arabian Sea is the second largest submarine fan in the world after the Bengal fan. Despite being an extensive physiographic and sedimentary feature, detailed mapping of the channel systems is very limited. Identification of five unreported deep sea channels using multibeam swath bathymetry data (collected by NCAOR) led to the outset of this study. Based on this survey in conjunction with the global seafloor topography data, here we present a GIS approach to report a "Projected Channel System" (PCS). Identification of the PCS is dependent on the calculation of flow direction. The values of flow direction raster range from 1 to 128, where 1 represents east; 4 depicts south; 16 is west and north is shown as 64. Subsequent calculation of flow accumulation and ordering of streams helped in marking major and minor streams. The method has successfully captured channel systems belonging not just to Indus drainage basin but several others, in an area of 3.03 x 10^6 km^2. Data from previously published channel systems – belonging to the Indus system were used to validate the results. Average offset distance between previously identified channels and PCS channels was ~10 km, indicating a reasonably good overlap.

Keywords *Multibeam Bathymetry; Flow Direction; Flow Accumulation; Stream Order; Projected Channel System*

1. Introduction

In this study the capability of GIS to identify deep sea channels, which are trough-shaped valleys of low relief occurring beyond the continental rise on the deep seafloor, has been discussed. These channels are formed by fast-flowing turbidity currents carrying terrigenous sediments. Channel levee complexes which are a result of deposition along the flanks of submarine channels; continental slopes and submarine canyons provide helpful insight to the identification of hydrocarbon reservoirs – their presence, quality and performance (Callow et al., 2014). Due to their economic significance, lithological studies of these depositional features have gained more impetus over the last 5 – 10 years (Mayall et al., 2006). As for the identification and interpretation, several tools have been developed so far. The implementation of "Hydrology" tools with respect to land based fluvial channels, is not a new concept and has yielded significant headway. Several previous studies performed by – Belknap and Naiman (1998); Cochrane and Flanagan (1999); Imaki and Beechie (2008) exemplify the implementation of GIS in hydrology. As was stated by Vieux (2001), GIS has become an integral part of hydrologic studies owing to the spatial character of parameters controlling hydrologic processes. It can hence be gathered that GIS based analyses have been performed in the past, withal, in the current study, authors wish to establish the credibility of GIS (in the marine context) for mapping deep sea channels in the Arabian Sea using global seafloor topography datasets.

A major thrust for pursuing this study came from the identification of five deep sea channels in the Laxmi basin during a survey for acquiring multibeam swath bathymetry data, by National Centre for Antarctic and Ocean Research (NCAOR) in 2013. The morphology of the channels indicated that they belonged to the *mature* stage of channel development. Since it is undisputable that submarine channels have a sediment source from a proximal terrestrial drainage system – a methodology was developed to map the entire channel network flowing in the Arabian Sea. This methodology includes key parameters like – flow direction, flow accumulation and stream order that shall be discussed in-depth.

After a cogitation of the channels within their network, basins were also delineated on the basis of channel flow direction and stream order. The results showed that the terrestrial Indus drainage basin is the most significant contributor of sediments to the Arabian Sea but, several other lesser order rivers flowing from the west coast of India, were also seen to contribute into this large drainage network.

Validating the resultant channel system was another crucial component of the study for which channels identified by Kodagali and Jauhari (1999) and Kenyon et al. (1995) were used, along with channels identified by NCAOR as previously mentioned. The comparisons affirmed that on an average, orthogonal distance measurement between the channels of PCS and the identified channels' thalweg was ~10 km. The final conclusions drawn from this work have shown the reliability of GIS techniques with special reference to *Hydrology tools* for studying marine channel systems.

2. Study Area

The identification of the PCS was done all along the latitudinal (3º N to 25º N) and longitudinal (64º E to 77º 30' E) extent of the Arabian Sea, i.e. from the Oman Abyssal Plain in the north to the Carlsberg Ridge in the south, flanked by the Indian and Oman coasts on either sides (Figure 1).

Three datasets of identified submarine channel systems (using ship borne data) were employed for validating the results of this study. Their extents have been marked as Block 1, 2, and 3 on Figure 1. Multibeam swath bathymetry data reported by Mishra et al. (2015), were acquired onboard *ORV Sagar Kanya* in 2013 having regional extent between 16º 00' 00'' N to 18º 12' 10'' N and 67º 53' 27'' E to 69º 49' 01'' E (Block 1). Channels identified by Kodagali and Jauhari (1999) extend between 12º 00' N - 13º 20' N and 66º 30' E - 69º 00' E, marked as Block 2. Also, channel levee complexes mapped by Kenyon et al. (1995) flowing between 14º 00' N to 24º 00' N and 62º 00' E - 68º 30' E is shown as Block 3.

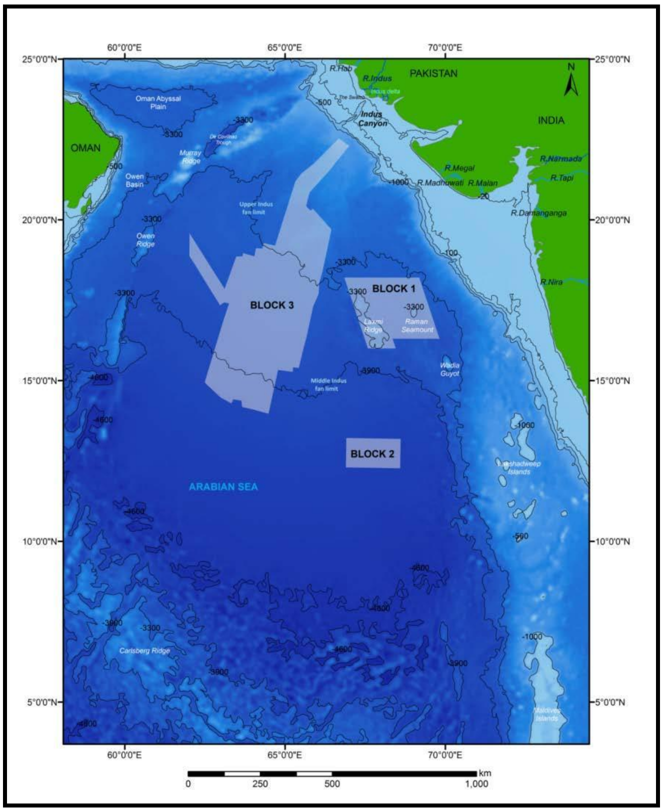

Figure 1: *Study Area with Block 1, 2 and 3 Indicating General Sea Floor Morphology of Arabian Sea and Western Indian Continental Shelf. Upper (-3300 M Contour) and Middle (-3900 M Contour) Indus Fan Limits have been Marked Indicating that Channels Identified in Block 1, 2 and 3 Belong to Middle, Lower and Upper-Middle Indus Fan Zones*

3. Materials and Methods

3.1. Data Specifications

In the entire study, four datasets have been employed. One is for creating the Digital Bathymetry Model (DBM) for the entire Arabian Sea, which has further been utilized for extraction of the PCS. Remaining three datasets were applied for the validation of the PCS.

3.1.1. Creation of DBM

The data employed for projecting the channel system was downloaded from http://topex.ucsd.edu/cgi-bin/get_data.cgi. This data belongs to v16.1 of the Global Bathymetric Model data, hereinafter referred as GBM data; compiled by Smith and Sandwell (1997). A multitude of depth soundings' datasets synthesized with high-resolution marine gravity information from the Geosat and ERS-1 spacecraft, led to the development of this widely cited global bathymetric data. From the entire extent of the GBM data used in the study, only 13.81% of the values were measured soundings while remaining 86.91% were interpolations from satellite altimetry (Figure 2). Nevertheless, moderate spatial coverage of ship-borne data especially within Block 1-3, aided in the generation of fairly accurate DBMs for the study.

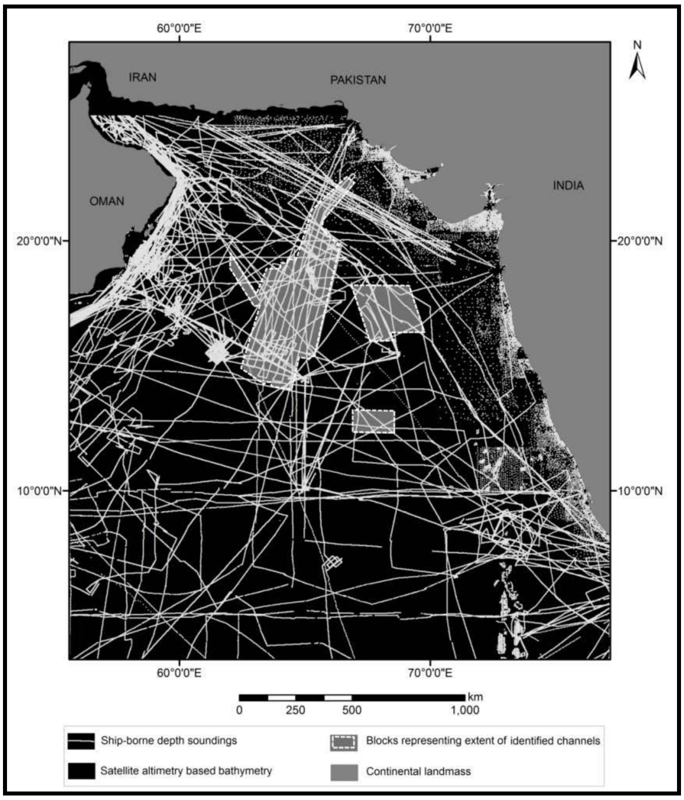

Figure 2: *Source of Global Bathymetry Model (GBM) Data Used for the Study (Smith and Sandwell, 1997). Area Shown in Black is Representing Satellite Altimetry Based Bathymetry; Zig-Zag Lines in White Represent Actual Ship-Borne Depth Soundings; While Three Gray Blocks with Dashed White Borders Mark out Regions Where Channels have been Identified Previously*

3.1.2. Validation of PCS

Three data sources were utilized for accuracy assessment of the PCS. These have been described below:

Dataset 1

Multibeam swath bathymetry data was acquired over an area of 54,253 km^2 onboard ORV Sagar Kanya using *SeaBeam 3012 Multibeam Echosounder*; a 12 kHz, 201 beam sonar system (~190 performing) with an effective swath of 90-140º at depths 3000 to 4000 m. DBM created using this data along with the identified channels (channel 1, 2, 3, 4A and 4B) is shown in Figure 3. 3D visualization of the prime features reported – Raman Seamount (RS) and Laxmi Ridge (LR), is depicted in Figure 4.

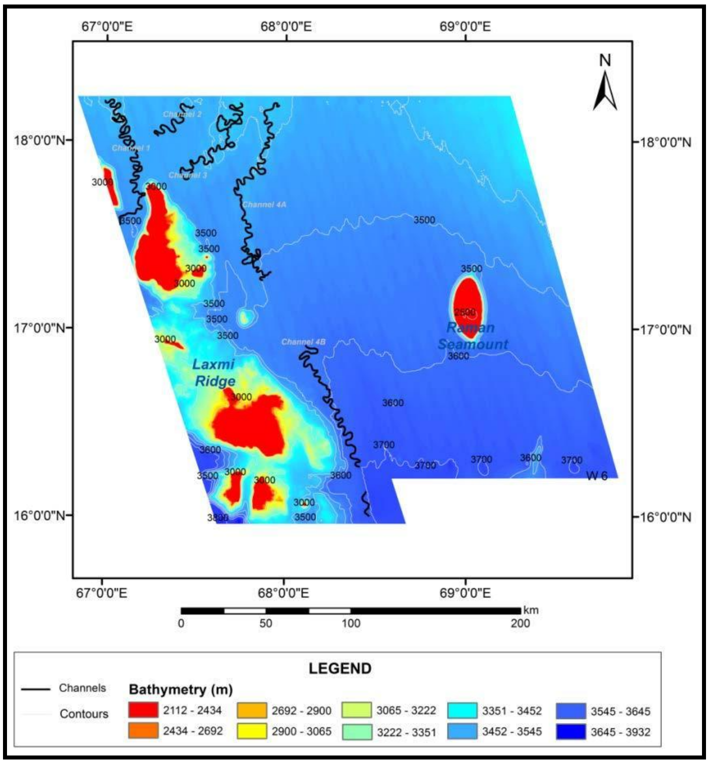

Figure 3: *Digital Bathymetry Grid Created Using Multibeam Swath Bathymetry Data. Identified Channels Marked as 1, 2, 3, 4A and 4B*

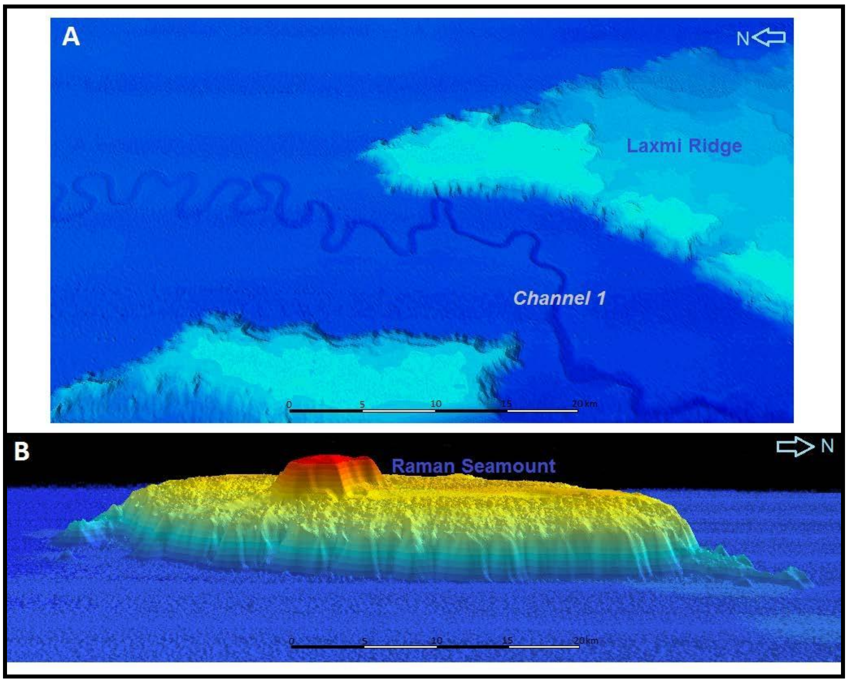

Figure 4: *(A) 3D Depiction of Channel 1 Flowing between the Northern Segments of the LR Seamount Chain and (B) RS. Highest Recorded Elevation of LR and RS was 835 M and 1371 m respectively*

Dataset 2

Data reported by Kodagali and Jauhari (1999) was collected using *Hydrosweep* multibeam swath bathymetry system (predecessor of *SB 3012*) onboard ORV Sagar Kanya; a 15.5 kHz system with 59 performed beams. The area covered in the survey approximated 18,600 km^2.

Dataset 3

Large channel-levee systems mapped by Kenyon et al. (1995) were captured in detail using long-range side-scan sonar GLORIA i.e. Geological Long Range Inclined Asdic (Rusby et al., 1973), spreading over an area of about 194,538 km^2. Interpretation of the GLORIA mosaic given by Prins et al. (2000) has been used in this study for mapping the channel systems.

The extents of dataset 1, 2, 3 have been respectively marked as Block 1, 2, 3 on Figure 1.

3.2. Methods

3.2.1. Processing of GBM data

Data downloaded in .xyz format (as shown previously in Figure 2) from Smith and Sandwell (1997) was converted into a continuous DBM covering the gamut of Arabian Sea. It was generated at a grid resolution of 1.7 x 1.7 km. Generation of DBM for the entire survey block demanded more than a simple interpolation due to the voluminous data involved. To deal with this, without compromising on the resolution of the bathymetric grid, generation of *terrain datasets* was performed. These are specifically suited for managing, processing and integrating massive point collections of 3D data collected from high resolution elevation observations, such as LiDAR, SONAR etc. (Childs, 2011). A terrain dataset is created by elevation soundings residing in a geodatabase to produce multi-resolution Triangular Irregular Network (TIN) based surfaces.

3.2.2. Identification of PCS from GBM data

Channel identification and subsequent basinal segregation, involved several steps, that have been discussed below:

Creation of Depression-Less DBM

Any surface representing the topography or bathymetry of a region may sometimes have unrealistic or erroneous sinks/depressions. As has been stated by Jenson and Domingue (1988), DEMs almost always contain depressions that hinder flow routing. It has also been noted previously that omission of such depressions has a positive influence on enhancing the quality of elevation models (Lin et al., 2008). Several techniques have been developed for eliminating these undesired sinks as discussed by Jenson and Domingue (1988), Fairfield and Leymarie (1991) and Garbrecht and Martz (1997). Li (2014) has portrayed the variation by observing profiles of cross sections in corrected and uncorrected DEMs.

These sinks may exist as single pixels or alternatively, as a group of multiple pixels with values lesser than all their surroundings pixels. The process to fill up these sinks may consequently, be direct or iterative in nature depending on the number of pixels involved. The DBM generated for the study area, was corrected for erroneous depressions. An optional z-limit value can be specified in order to define the maximum depth of a sink that must be filled. The most profound difference between the filled and unfilled DBM can be appreciated only when flow accumulation is calculated (detailed discussion in section *3.2.2 c.*). For comparison purposes, flow accumulation was assessed using an uncorrected section of the DBM, results of which can be seen in Figure 5.

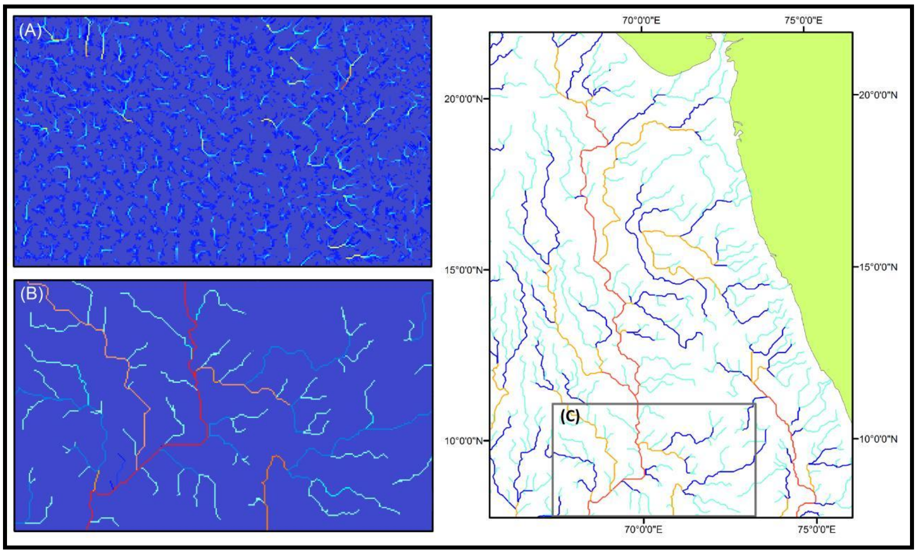

Figure 5: *Flow Accumulation Calculated On (A) Uncorrected DBM and (B) Depression-Less DBM; Block Represents Location of the Area Shown in the Comparison*

Calculation of Flow Direction

The second step involves the computation of a flow direction raster, which shows the *direction* of the steepest flow of water from each cell to its adjoining cells. This determination of flow direction is performed using the D8 algorithm postulated by O'Callaghan and Mark (1984). The values depicting direction of flow range from 1 to 128, starting from the east incrementing clockwise. The values are coded as powers of 2 from 0 to 7, i.e. 2^0 = 1; 2^1 = 4 and 2^7 = 128, in order to make the surround conditions correspond to unique values, when the powers of two are summed for any unique set of neighbours (Jenson and Domingue, 1988). The directions and output of flow direction for the study area is shown in Figure 6.

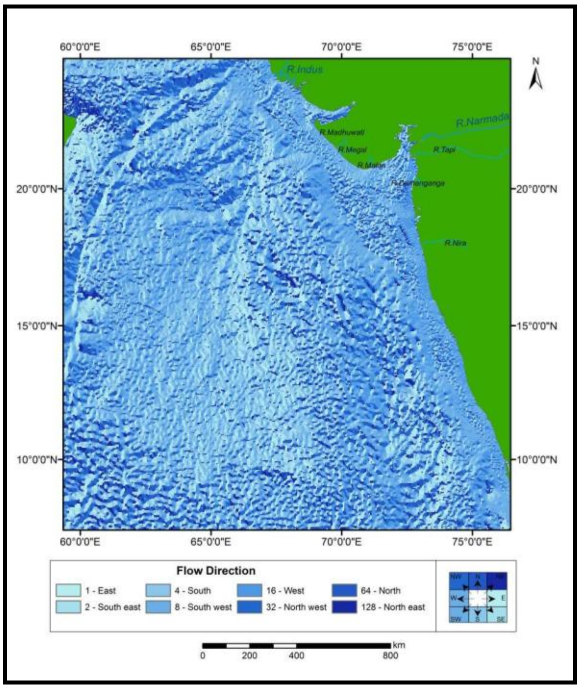

Figure 6: *Flow Direction across the Arabian Sea Shown in 8 Colours Derived from D8 Algorithm (O'Callaghan and Mark, 1984) Representing 8 Cardinal Points*

There can be several different scenarios prevailing within an area, each needing a conditional approach to identify flow direction. Conditions where the elevation of the central pixel is lesser than its surrounding cells *in toto,* the flow direction would be encoded as negative since it cannot be defined. However, for computational purposes, these cells are considered and assigned the value of their lowest elevation neighbour. Such cases may be rare especially after obviating the erroneous sinks. The second condition, also the most common, would be when the elevation drop is greatest in only one direction from the central cell. For instance, if the elevation of the pixel to the right of the central cell is lesser than all the other seven adjacent ones i.e. the steepest flow is towards right, the flow direction assigned to that cell would be 1 (east flow). Alternatively, issues arise when the same change in z-value is observed in multiple directions. In cases where three adjacent pixels along one edge exhibit equal drops in elevation, the central cell can be chosen and assigned the flow direction. If two cells on opposite sides have equal z-value, either of the two directions can be arbitrarily chosen or with a lookup table defining the most likely direction. A distance weighted drop raster can also be calculated that depicts the ratio of the maximum change in elevation from each cell along the direction of flow to the path length between centers of cells, expressed in percentages. Computation of the flow direction raster must be as accurate as possible, since it is the main input for assessing flow accumulation and subsequent stream flow analysis.

Identification of Flow Accumulation

Next, a raster displaying the flow accumulation is derived from the flow direction. Here each pixel represents the cumulative number of cells that flow into it from all directions. The value of accumulated flow increases on going downstream along any given channel, while reduces upstream. Flow accumulation analysis is significant for identifying stream channels because higher accumulation would directly imply greater contribution of flow from surrounding cells. There is no fixed range of flow accumulation values, since the values continue to increment downslope with the length of the stream channel, however, there can be “zero” values indicating pixels which do not have any cells flowing in to them. The zero valued cells do not contribute to any downstream flow and are mostly found to be local topographic highs. The output can be user defined as integer or float values.

Flow direction and Flow accumulation tools, available with the Hydrology tools of the ArcGIS 10.1 package, gave promising results by closely estimating the pattern and accumulation of drainage channels in the study area.

Filtration of Flow Accumulation Raster

Several stream channels can be arrived at from the preceding step; however, not all of them may be valid participants to the drainage network. In order the deduce only the principal streams, a logical and locally applicable threshold can be defined to filter the flow accumulation raster resulting into a binary inferred stream raster, where 0 would represent “no flow” and 1 represents “stream flow”. Simple conditional tools of CON or SETNULL (Spatial Analyst tools) can be implemented to obtain such binary stream flow representing raster datasets. The optimum threshold value, as previously mentioned, is local in nature and must be tried on the data repeatedly – higher the value lesser the density of the drainage network and vice versa. Once the principal streams are classified, other ephemeral streams may be progressively included by reducing the threshold (Mackenzie, 2004).

In the current study, after carefully observing the histogram distribution and repeated trials with the threshold value, the satisfactory binary stream flow raster was obtained. If the focus is on extracting the prime channels, without ignoring the consequent and subsequent streams, this step is quickly executable. Also, another parameter considered to optimize the threshold, was to fine tune the value that could surface the channels identified by previous surveys (shown in Block 1-3, Figure 1).

Ordering of Streams

Once the binary raster denoting stream network has been precisely deduced from flow accumulation data, an integer value raster can be obtained by implementing the Stream Order tool. As shown in Figure 7, two ordering methods namely, Strahler (1952) and Shreve (1966) have been discussed in this study.

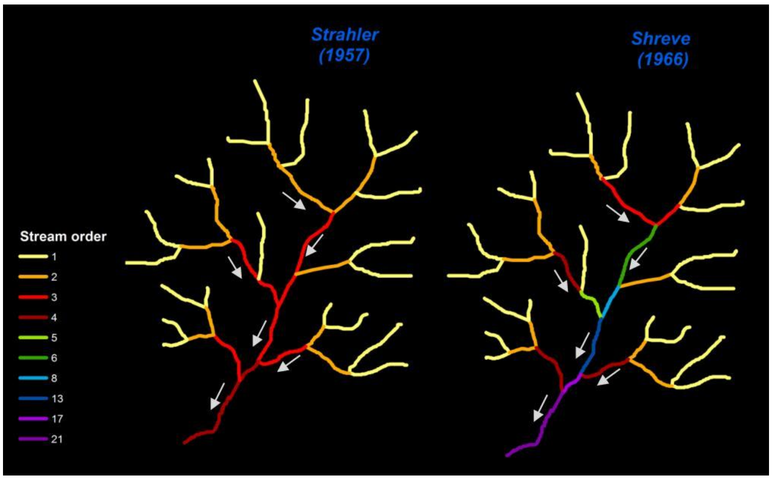

Figure 7: *A Comparison of Stream Order Methods by Strahler (1952) and Shreve (1966). In the Illustration it can be Observed That a Stream in the Higher Order of 4 (Strahler) Becomes 21 in Shreve's Model Hence Depicting the Additive Approach of the Latter*

Since Shreve's method grows additively considering each and every interior link of the system as opposed to Strahler's method; it would have resulted in extremely high order streams towards the lower reaches of the channel network. It is also stated that numbers from the Shreve method refer to magnitudes instead of orders (magnitude representing the total number of upstream links). Because the quantum of streams identified was immense in the study area, Shreve's cumulatively growing stream order method could have produced exaggerated results. On the other hand, Strahler's technique helped in suitably picking out the major/principal channels which were also found to be spatially associated with some or the other river delta network on land (discussed later). The streams so acquired can be easily converted to vector format as it supports easier clean-up of the data and ensures correct connectivity and directionality.

Basinal Delimitation

Finally, the flow direction raster was subsequently used to differentiate between the multiple basins existing within the area of study. Here, all streams that flow into a common basin are circumvented to belong to one unique drainage basin. These can be later merged so as to attain only broad basinal margins and ignore sub-watersheds.

3.2.3. Validation of the Projected Channel System

Three sources of identified deep sea channels were employed to validate the network acquired by the aforementioned techniques. Channels from the PCS were spread out all across the breadth of the Arabian Sea. Most of the channels initiating from the landward area were found to be at proximal distances to major/minor river systems, for e.g. those from R. Indus and R. Narmada and also from R. Hab, R. Mol Nadi (Pakistan); R. Damanganga, R. Madhuwati, R. Megal etc. (India).

The channels used to validate the PCS have been shown in Figure 8. Channels identified by Mishra et al. (2015) extracted from multibeam swath bathymetry data belonged to the middle Indus fan region. In the lower Indus fan, Kodagali and Jauhari (1999) identified five distinct meandering channels at the water depth of 4200 m; however, they appear to be missing in a few sections perhaps due to data loss. Kenyon et al. (1995), while working on the geometry of younger sediment bodies in the Indus fan observed several large channel levee complexes, which have also been used for corroboration.

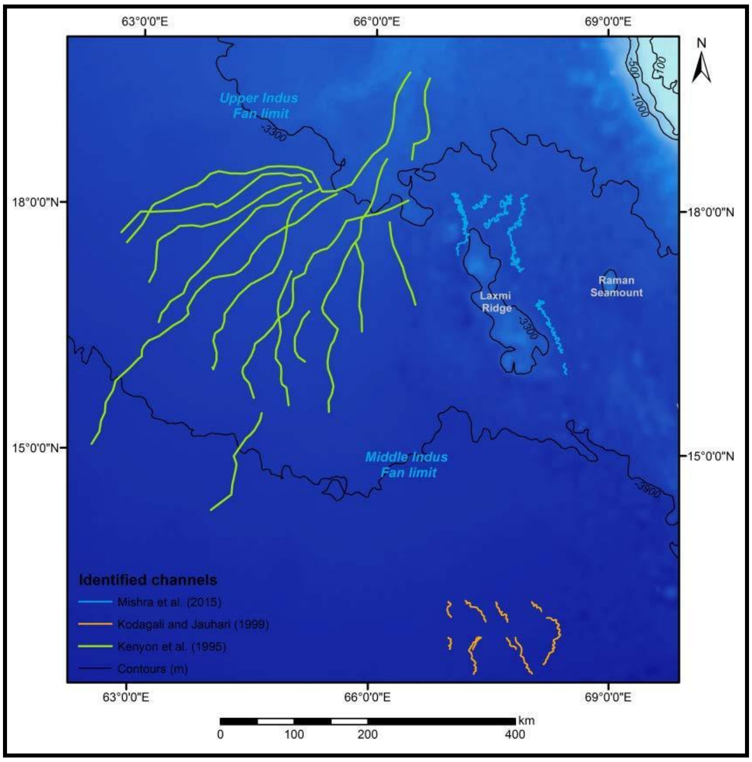

Figure 8: *Identified Channels Implemented in the Study for Validating Results of PCS (Mishra et al., 2015; Kodagali and Jauhari, 1999; and Kenyon et al., 1995)*

A straight forward yet statistically sound measure to check the spatiality of the channels derived from GBM data was to construct orthogonal sections from the previously identified channels' thalweg to the channels of PCS. In all, ~400 such sections were created at equal intervals along the channels, on the basis of which an average offset value was achieved.

4. Results and Discussion

Channels identified in Block 1 (Figure 1 and Figure 2) were delineated from multibeam swath bathymetry data. To facilitate understanding of their morphometric behaviour; length, width and depth calculations were made using ArcMap 10.1. These have been discussed by Mishra et al. (2015), but to summarize here, the depth of the channel mostly ranged around 60 m. To portray the nature of the channel valley, several cross profiles were constructed running across either banks of the channel trunk.

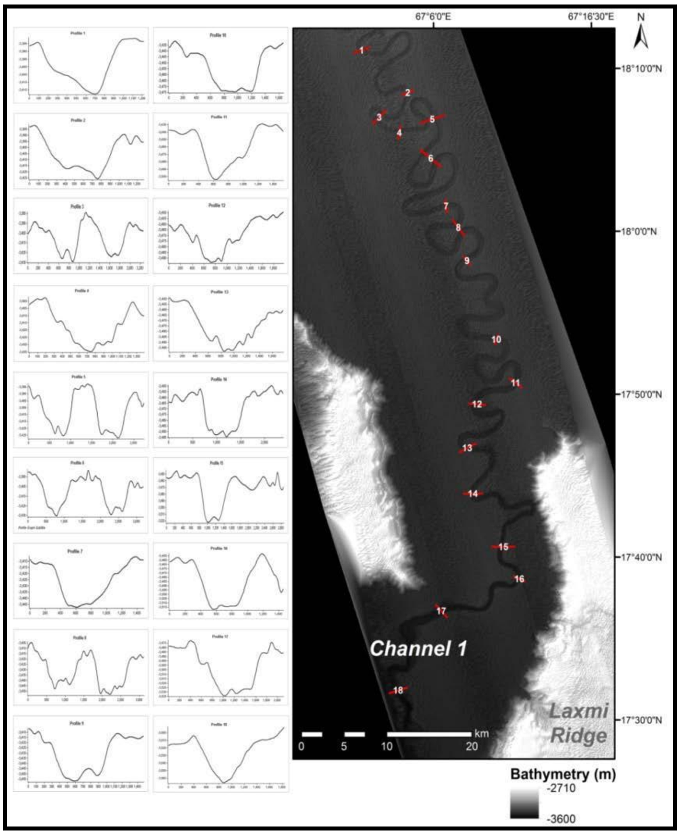

Figure 9: *Cross Sectional Profiles are drawn along the Course of Channel 1 That Runs Amidst the North-Western Segment of the Laxmi Ridge Chain (Location of Channel 1 Can Be Seen in Figure 2). The Bathymetry Shown in the Right Panel Ranges from 2710-3600 m. The Depth of Channel 1 was found to Vary from 59.75 to 82.23 m Incising More from North to South. The Deeper Gray Shades of the Channel Notable in Profiles 11 to 18 are Indicative of Increasing Channel Depth*

As can be concluded from Figure 9, at most cross sections, a U-shaped valley exists. Along with that, distinguished meandering observed at several locations along the course of the channels, are indicative of mature stage of development. However, no ox-bow lake formations were noted. The presence of the channels in the middle Indus fan region suggested their affiliation to drainage systems originating from the proximal continental shelves. Hence, this study was performed to extrapolate the channels and project the complete drainage network of the Arabian Sea basin.

Methodology discussed in section 3.2.2 resulted in the identification of a "projected channel system" using Hydrology tools in a GIS framework. The entire stream network of the derived PCS has been exhibited in Figure 10.

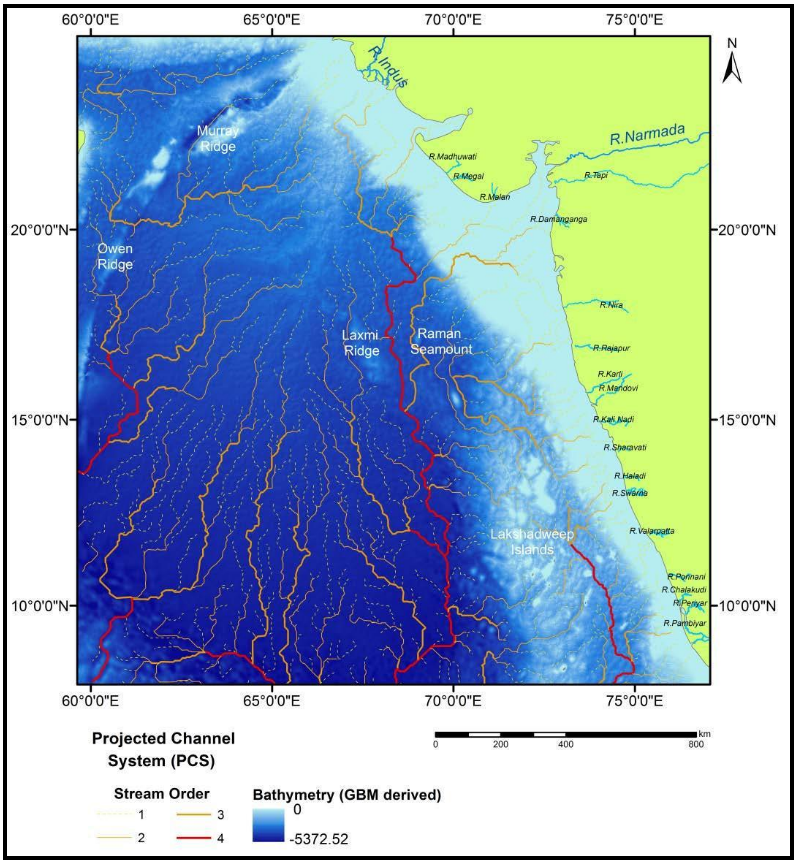

Figure 10: *Projected Channel System (PCS) of the Arabian Sea Indicated using Strahler's Method of Stream Order, Ranging from 1-4*

Ordering of the streams further elevated the study to support the identification of major channels flowing in from land making their way through the abyssal plains. From what came out in the result of this exercise, apart from R. Indus and its enormous delta flowing into the north eastern Arabian Sea, there were several other participants contributing to the flow of channels in the study region. Numerous minor river systems draining from the western Indian coastline could perhaps, have an influence on the stream flow noticeable on the adjacent continental shelf. Since most of them were first order streams (commencing from the continental shelves), they were subsequently seen to merge with more streams leading to the emergence of higher order channels. One of the most significant channel systems running from the Indus canyon up till the Carlsberg Ridge, in a north-south trend, has been marked in Figure 10. Its continual flow and a profound tributary structure assert that the drainage network is well developed. Also, the channels of the PCS along with their tributaries form dendritic patterns occurring mostly in flat-lying surfaces with homogenous material, as is in the case of abyssal plains.

In order to associate the streams with their potential antecedent sources, a categorization of the entire drainage basin was done. This basinal classification of the Arabian Sea resulted in demarcation of several sub-basins (Figure 11). The divisions of the drainage basins were again based on the flow direction parameters. Streams draining into a common exit point were engulfed to denote participation to only one drainage basin. Also, no single stream is seen to drain into two or more different basins.

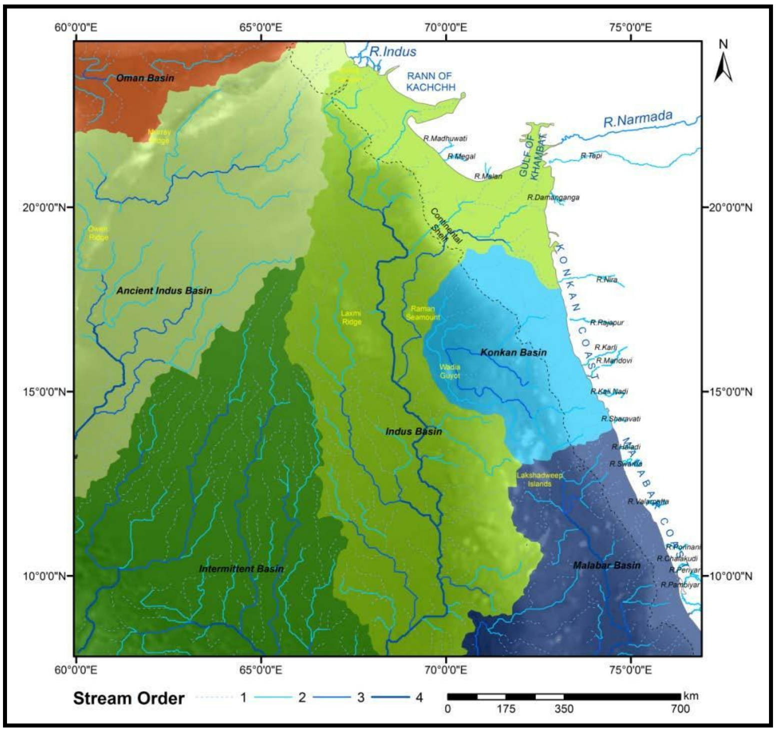

Figure 11: *Basinal Classification of the Arabian Sea Overlain By PCS. 6 Basins Have Been Identified Namely – Indus, Intermittent, Ancient Indus, Malabar, Konkan and Oman Basin (In Descending Order of their Areas). R. Indus is The Principal Contributor of Sediments to the Arabian Sea Drainage Network Thereby Having the Greatest Drainage Basin*

In all, six distinct basins could be delineated, with the largest being *Indus basin* covering 9.3 x 10^5 km^2. Contribution of smectite rich sediments from R. Narmada and R. Tapti into the Arabian Sea has been previously reported (Ramaswamy et al., 1991). Smectite rich sediments are seen to be prevalent in greater proportions only in the Central and Eastern Arabian Sea, though most of it is deposited on Western continental shelf. On the other hand, illite rich sediments brought in from R. Indus is the most prominent mineral in the Arabian Sea (Konta, 1985). Since the contributions from R. Narmada and R. Tapti are significantly low as opposed to the illite rich sediments belonging to the Indus river system, in this study the basin has been denoted as *Indus Basin*.

Deptuck et al. (2003) identified an ancestral Indus canyon existing to the north-west of the modern day Indus canyon. Although the modern Indus canyon is a feeder to the Indus basin demarcated in this study, an equally dense network of channels egressing from its ancestral counterpart can be identified – marked as *Ancient Indus Basin*. Young channel – levee complexes determined by Kenyon et al. (1995), also belong to this drainage basin.

In between the two R. Indus fed basins, lies an enormous channel system marked as the *Intermittent Basin* named so due to its disassociation with adjacent basins. On the north-north western portion of the Arabian Sea is the *Oman Basin* with its own distinct drainage network. With no intermingling of its channels to the *Ancient Indus Basin*, attributable to the Murray Ridge, Qalhat seamount (SW of Murray Ridge) and De Covilhao Trough, its channels run in an east-west trend collaborating with those from the Owen Basin further south.

Coming to the smaller river systems feeding the channels of the *Konkan* and *Malabar Basins*, several streams can be seen to branch out into the Arabian Sea. Only a few significant rivers of south west India have been marked in Figure 11 however, a much greater density of rivers exists in the area. The spatial extent of the respective basins has been given in Table 1.

Table 1: *Identified Basins with Their Respective Area*

Basin	Area (km^2)
Indus Basin	934343
Intermittent Basin	689359
Ancient Indus Basin	614726
Malabar Basin	314597
Konkan Basin	247490
Oman Basin	152428

Validation of the PCS: As previously stated, orthogonal distances were measured to assess the distance between the identified channels' thalweg and the channels of the PCS. A total of 391 sections were created, a sample of which can be seen in Figure 12, from all the channels described by Mishra et al. (2015), Kodagali and Jauhari (1999) and Kenyon et al. (1995). The lengths of these sections ranged from ~30 km to being as small as a few hundred meters (Figure 13). An average distance representing the *offset* between the two different channels was found to be 10.35 km using this method. Considering the gigantic spread of the Arabian Sea basin with its seamless drainage network, a spatial drift of this measure was reckoned to be justifiable.

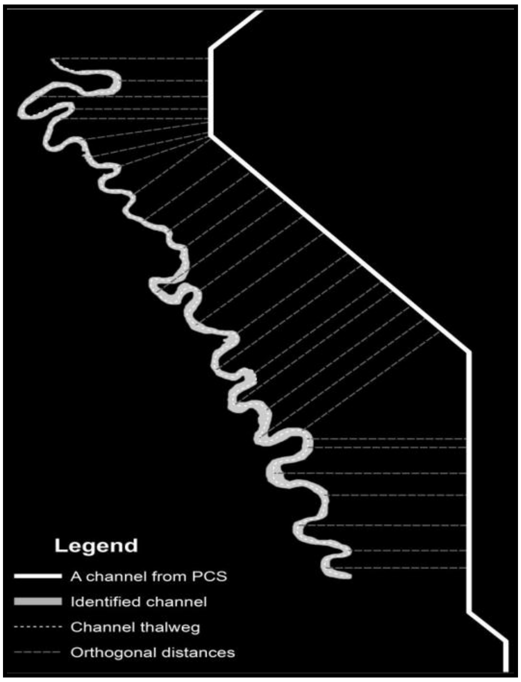

Figure 12: *An Illustration of the Validation Technique Followed in the Study. Orthogonal Distances (Dashed Lines) have been Measured at 391 Places Connecting the Respective Thalwegs of Identified and Projected Channels*

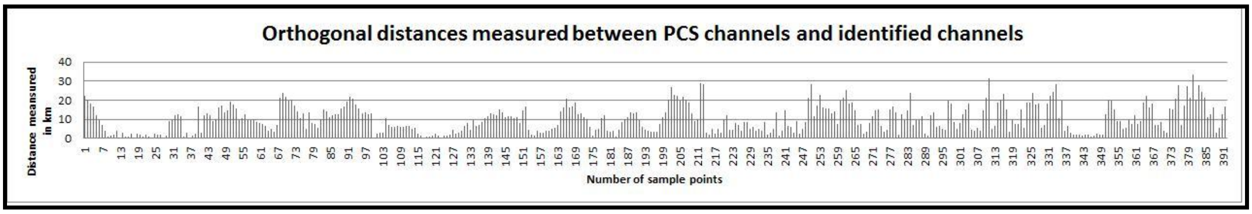

Figure 13: *Graph Indicating the Variation in Orthogonal Distances Across 391 Sections Created to Calculate the Offset Error. The Average Offset Value was 10.35 Km with Minimum Being 0.16 Km and Maximum 33.37 Km*

5. Conclusion and Future Scope

Submarine canyons are established sources of feeding channel levee complexes. Dense turbidite currents carrying slurries of terrigenous sediments create deep indents on the continental shelves, which over time shape up as submarine canyons. These sediments locomote themselves from the land-sea interface to the abyssal plains via arteries of submarine channel networks. Largest accumulations of terrigenous sediments created at the termini of continental landmasses are hence created in the form of submarine fans. The Indus canyon (shown in Figure 14), a relic feature from the pre-Holocene relief (Inam et al., 2007) is the prime catalyst of the modern day Indus basin. This is because of its preventive role played in the development of the subaqueous Indus delta, causing the sediments to be funneled towards the submarine fan (Islam, 1959; Nair et al., 1982; Wells and Coleman, 1984). The exposure of the sub-aerial continental shelf during the Quaternary low sea levels, led to the progression of channels of the Indus River on the shelf, causing the development of the Indus canyon (Inam et al., 2007). Also, deposition of the sediments on the upper slope of the canyon produced from turbidity currents and backward erosion from mass wasting processes further led to the carving of the canyon during glacial and interglacial periods. It is commonly held that sedimentation is focused on the inner shelf during highstands and conversely on the fan during lowstands (Haq et al., 1987). But in the case of Indus, this has been held partly unlikely (Burgess and Hovius, 1998) because delta progradation took place as a faster rate as compared to the duration of third order sea level highstands. Therefore, it was concluded by Clift et al. (2002) that even during the highstands, sediment is supplied to the Indus canyon and further deposited on the deep basin.

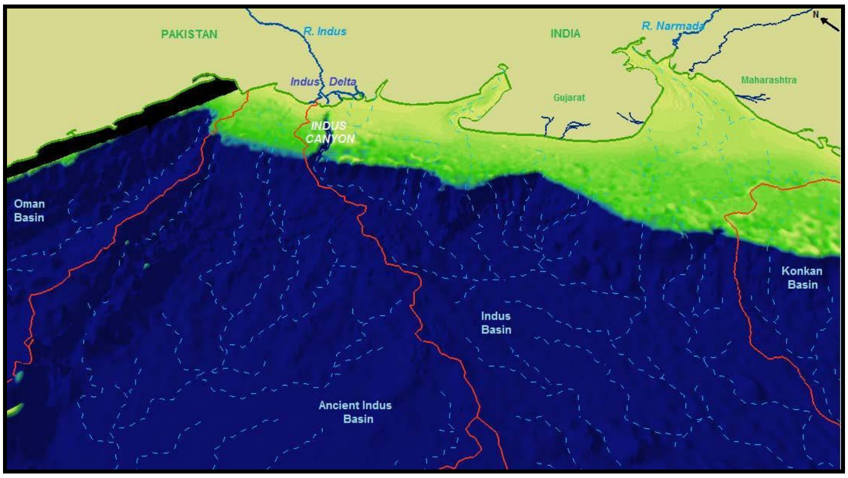

Figure 14: *3D View of the North Western Continental Shelf of India Indicating Modern Day Indus Canyon, The PCS (Dashed Blue) and the Proximal Basins (Red Boundaries)*

In context to the current study, previous works supported by seismic records on the shelf (Kolla and Coumes, 1987) have already established the occurrence of three marked canyons in the north western realm of the Arabian Sea. Concomitantly, the occurrence of several submarine channels in the region would be demonstrable, and this is what has been substantiated through this study.

The central focus of this work is to highlight the capacity of GIS tools for efficiently extracting deep sea channels from satellite derived/multi-beam swath bathymetry data. It is agreed that satellite bathymetry data is not always a very reliable source for mapping deep sea channels especially in resolving those which are in order of only a few meters in width. However, this approach substantiates the implementation of GIS tools for studying such intricate flow patterns on seafloor topography in the absence of adequate high resolution data. Several automated models of stream/channel identification can be developed depending on the quality of the DBMs being used. Augmentation of more and more ship sounding based DBMs can provide greater accuracy in terms of mapping the deep sea channels.

This work also brings forth a new estimation of the patterns of flow and accumulation within the Arabian Sea and marks the contribution of several lesser order streams into the vast drainage expanse prevalent on the seafloor. The sediment influx into the Arabian Sea from the Indus River has been established over decades supported with bathymetric, seismic and sedimentological data but the channels emerging from the western coast of India wedging their way through the continental shelf and subsequently contributing to the channel network of the Arabian Sea makes this study different from others. This is a first such attempt to conjugate all contributors of sediment into this world's second largest submarine canyon also indicating their route and stream order. The basinal classification discussed above also incites the understanding of the direction of flow prevalent on the seafloor. A detailed study of individual basins along with their extended land based counterparts can reveal several facts about the sediment flow, their velocity, run off rates, volume, composition etc.

This study hence, provides a rudimentary base for future studies involving more detailed analyses of these complex structures. Several researchers in the past have interpreted channels and their levee complexes using multi-channel seismic reflection data (Clift et al., 2002; Bourget et al., 2013). With the inclusion of more bathymetric and seismic interpreted data to identify buried/passive channels, the results of this study can be refined further. Also, the methodologies and techniques discussed herein can be applied onto regions where ship sounding data acquisition may not be possible.

Acknowledgment

The authors would like to thank Director, National Centre for Antarctic and Ocean Research, for providing continued support to carry out this study. Authors also express their gratitude to Dr. Walter H.F. Smith for his valuable suggestions. The diligent service provided by Master and crew of ORV Sagar Kanya is also thankfully acknowledged. This is NCAOR Contribution No. 22/2015.

References

Belknap, W. and Naiman, R.J. *A GIS and TIR Procedure to Detect and Map Wall-Base Channels in Western Washington.* Journal of Environmental Management. 1998. 52 (2) 147-160.

Bourget, J., Zaragosi, S., Rodriguez, M., Fournier, M., Garlan, T. and Chamot-Rooke, N. *Late Quaternary Megaturbidites of the Indus Fan: Origin and Stratigraphic Significance.* Marine Geology. 2013. 336; 10-23.

Burgess, P.M. and Hovius, N. *Rates of Delta Progradation during Highstands; Consequences for Timing of Deposition in Deep-Marine Systems.* 1998. In: Clift, P.D., Gaedicke, C., Edwards, R., Lee, J.I., Hildebrand, P., Amjad, S., White, R.S. and Schlüter, H.-U. *The Stratigraphic Evolution of the Indus Fan and the History of Sedimentation in the Arabian Sea.* Marine Geophysical Researches. 2002. 23 (3) 223-245.

Callow, R.H.T., Kneller, B., Dykstra, M. and McIlroy, D. *Physical, Biological, Geochemical and Sedimentological Controls on the Ichnology of Submarine Canyon and Slope Channel Systems.* Marine and Petroleum Geology. 2014. 54; 144-166.

Childs, C. *Terrain Datasets: The Top 10 Reasons to Use Them.* ArcUser Online, Spring Edition 2011. http://www.esri.com/news/arcuser/0311/terrain-datasets.html

Clift, P.D., Gaedicke, C., Edwards, R., Lee, J.I., Hildebrand, P., Amjad, S., White, R.S. and Schlüter, H.U. *The Stratigraphic Evolution of the Indus Fan and the History of Sedimentation in the Arabian Sea,* Marine Geophysical Researches. 2002. 23 (3) 223-245.

Cochrane, T.A. and Flanagan, D.C. *Assessing Water Erosion in Small Watersheds using WEPP with GIS and Digital Elevation Models.* Journal of Soil and Water Conservation. 1999. 54 (4) 678-685.

Deptuck, M.E., Steffens, G.S., Barton, M. and Primez, C. *Architecture and Evolution of Upper Fan Channel-Belts on the Niger Delta Slope and in the Arabian Sea.* Marine and Petroleum Geology. 2003. 20; 649-676.

Fairfield, J. and Leymarie, P. *Drainage Networks from Grid Digital Elevation Models.* Water Resources Research. 1991. 27 (5) 709-717.

Garbrecht, J. and Martz, L.W. *The Assignment of Drainage Direction over Flat Surfaces in Raster Digital Elevation Models.* Journal of Hydrology. 1997. 193 (1-4) 204-213.

Haq, B.U., Hardenbol, J. and Vail, P.R. *Chronology of Fluctuating Sea Levels since the Triassic.* 1987. In: Clift, P.D., Gaedicke, C., Edwards, R., Lee, J.I., Hildebrand, P., Amjad, S., White, R.S. and Schlüter, H.U. *The Stratigraphic Evolution of the Indus Fan and the History of Sedimentation in the Arabian Sea,* Marine Geophysical Researches. 2002. 23 (3) 223-245.

Imaki, H. and Beechie, T. *GIS Approaches for Channel Typing in the Columbia River Basin: Carrying Fine Resolution Data to a Large Geographic Extent.* American Geophysical Union, Fall Meeting 2008. Abstract no H51A-0789. http://adsabs.harvard.edu/abs/2008AGUFM.H51A0789I.

Inam, A., Clift, P.D., Giosan, L., Tabrez, A.R., Tahir, M., Rabanni, M.M. and Danish, M., 2007: *The Geographic, Geological and Oceanographic Setting of the Indus River.* Large Rivers: Geomorphology and Management, Chapter 16, John Wiley & Sons, Ltd. 333-346.

Islam, S.R. *The Indus Submarine Canyon.* 1959. In: Inam, A., Clift, P.D., Giosan, L., Tabrez, A.R., Tahir, M., Rabanni, M.M., Danish, M., 2007: *The Geographic, Geological and Oceanographic Setting of the Indus River,* Large Rivers: Geomorphology and Management, Chapter 16, John Wiley & Sons, Ltd. 333-346.

Jenson, S.K. and Domingue, J.O. *Extracting Topographic Structure from Digital Elevation Data for Geographic Information System Analysis.* Photogrammetric Engineering and Remote Sensing. 1988. 54 (11) 1593-1600.

Kenyon, N.H., Amir, A. and Cramp, A. *Geometry of the Younger Sediment Bodies of the Indus Fan.* 1995 In: Prins, M.A., Postma, G., Cleveringa, J., Cramp, A., Kenyon, N.H. *Controls on Terrigenous Sediment Supply to the Arabian Sea During the Late Quaternary: The Indus Fan.* Marine Geology. 2000. 169 (3-4) 327-349.

Kodagali, V.N. and Jauhari, P. *The Meandering Indus Channels: Study in a Small Area by the Multibeam Swath Bathymetry System – Hydrosweep.* Current Science. 1999. 76 (2) 240-243.

Kolla, V. and Coumes, F. *Morphology, Internal Structure, Seismic Stratigraphy, and Sedimentation of Indus Fan.* AAPG (American Association of Petroleum Geologists) Bulletin. 1987. 71 (6) 650-677.

Konta, J. *Mineralogy and Chemical Maturity of Suspended Matter in Major Rivers Samples Under the SCOPE/UNEP PROJECT.* 1985 In: Ramaswamy, V., Nair, R.R., Manganini, S., Haake, B. and Ittekkot, V. *Lithogenic fluxes to the deep Arabian Sea measured by sediment traps,* Deep Sea Research. 1991. 38 (2) 169-184.

Li, Z. *Watershed Modeling Using Arc Hydro Based on DEMS: A Case Study in Jackpine Watershed,* Environmental Systems Research. 2014. 3 (11).

Lin, W.T., Choub, W.C., Lin C.Y., Huang, P.H. and Tsai, J.S. *Win Basin: Using Improved Algorithms and the GIS Technique for Automated Watershed Modelling Analysis from Digital Elevation Models.* International Journal of Geographical Information Science. 2008. 22 (1) 47-69.

Mackenzie, J. *Using ArcGIS Hydrology Tools to Model Watershed-Level Non-Point Pollution Management Strategies.* 2004. In: GIS in Natural Resource Management-Spring 2014 Course Syllabus, APEC/CANR. University of Delaware. http://www.udel.edu/johnmack/frec480/arc_watershed/.

Mayall, M., Jones, E. and Casey, M. *Turbidite Channel Reservoirs - Key Elements in Facies Prediction and Effective Development.* 2006. In: Callow, R.H.T., Kneller, B., Dykstra, M. and McIlroy, D. *Physical, Biological, Geochemical and Sedimentological Controls on the Ichnology of Submarine Canyon and Slope Channel Systems.* Marine and Petroleum Geology. 2014. 54; 144-166.

Mishra, R., Pandey, D.K. and Prerna, R. *Active Channel Systems in the Mid- Indus Fan: Results from the new High Resolution Bathymetry Surveys.* Current Science. 2015. 108 (3) 409-412.

Nair, R.R., Hashimi, N.H. and Purnachandra Rao, V. *On the Possibility of High-Velocity Tidal Streams as Dynamic Barriers to Longshore Sediment Transport: Evidence from the Continental Shelf off the Gulf of Kutch, India.* 1982. In: Inam, A., Clift, P.D., Giosan, L., Tabrez, A.R., Tahir, M., Rabanni, M.M., Danish, M., 2007: *The Geographic, Geological and Oceanographic Setting of the Indus River,* Large Rivers: Geomorphology and Management, Chapter 16, John Wiley & Sons, Ltd. 333-346.

O'Callaghan, J.F. and Mark, D.M. *The Extraction of Drainage Networks from Digital Elevation Data.* Computer Vision, Graphics and Image Processing. 1984. 28; 323-344.

Prins, M.A., Postma, G., Cleveringa, J., Cramp, A. and Kenyon, N.H. *Controls on Terrigenous Sediment Supply to the Arabian Sea During the Late Quaternary: The Indus Fan.* Marine Geology. 2000. 169 (3-4) 327-349.

Ramaswamy, V., Nair, R.R., Manganini, S., Haake, B., and Ittekkot, V. *Lithogenic Fluxes to the Deep Arabian Sea Measured by Sediment Traps.* Deep Sea Research. 1991. 38 (2) 169-184.

Rusby, J.S.M, Somers, M.L., Revie, J., McCartney, B.S. and Stubbs, A.R. *An Experimental Survey of a Herring Fishery by Long-Range Sonar.* Marine Biology. 1973. 22 (3) 271-292.

Shreve, R.L. *Statistical Law of Stream Numbers.* The Journal of Geology. 1966. 74 (1) 17-37.

Smith, W.H.F. and Sandwell, D.T. *Global Sea Floor Topography from Satellite Altimetry and Ship Depth Soundings.* Science. 1997. 277; 1957-1962.

Strahler, A.N. *Hypsometric (Area-Altitude) Analysis of Erosional Topology.* Geological Society of America Bulletin. 1952. 63 (11) 1117-1142.

Vieux, B.E. *Distributed Hydrologic Modeling Using GIS.* Water Science and Technology Library. 2001. 38; 1-17.

Wells, J.T. and Coleman, J.M. *Deltaic Morphology and Sedimentology, with Special Reference to the Indus River Delta.* 1984. In: Inam, A., Clift, P.D., Giosan, L., Tabrez, A.R., Tahir, M., Rabanni, M.M., Danish, M., 2007: *The Geographic, Geological and Oceanographic Setting of the Indus River,* Large Rivers: Geomorphology and Management, Chapter 16, John Wiley & Sons, Ltd. 333-346.